International Journal of Heat and Mass Transfer 52 (2009) 5229–5240

Contents lists available at ScienceDirect

International Journal of Heat and Mass Transfer

journal homepage: www.elsevier.com/locate/ijhmt

Modeling of the fluctuating component in the form of the sum of an infinite number of random quantities. Part 2. Model of transfer of turbulent stresses and turbulent heat fluxes

B.P. Golovnya

Department of Applied Mathematics, Cherkassy National University, 79 Shevchenko Blvd., Cherkassy 18013, Ukraine

ARTICLE INFO

Article history:
Received 24 January 2008
Accepted 14 July 2008
Available online 10 June 2009

Keywords:
Turbulence modeling
Turbulent stresses modeling
Turbulent heat flux modeling
Backward-facing step flow simulation

ABSTRACT

The paper presents an approach to construction of turbulence models that allows modeling of the fluctuating component in the form of the sum of an infinite number of random quantities. The first part of the paper deals with the technique of construction of the k-ε type model. In the second part of the paper, construction of the model of transfer of turbulent stresses and heat fluxes is considered. It is shown that the technique does not depend on the choice of the dissipative variable.

1. Introduction

In [1], the author suggested an approach to construction of turbulence models, which allows modelling of fluctuating components in the form of an infinite sum of random quantities. In this case, turbulence is modeled in the form of an infinite sum of vortex systems and the turbulence energy as a sum of an infinite number of energies. Vortex systems were given the names of primary, secondary, etc. It is assumed that only primary vortices interact with the mean flow. Each subsequent system arises as a result of the contact of the previous system with the wall and/or shear. We note that this theory is confirmed by experimental data.

The k-ε-type model of turbulence for calculation of the energy of primary vortices in the case of boundary-layer flow, which is developed on the basis of the suggested theory, has the form

$$\begin{cases} \frac{Dk_0}{D\tau} = f_0 \frac{\partial}{\partial x_k}\left(\nu + \frac{\nu_{0i}}{C_k}\right)\frac{\partial k_0}{\partial x_k} + f_0 P - \varepsilon_0, \\ \frac{D\varepsilon_0}{D\tau} = f_0 \frac{\partial}{\partial x_k}\left(\nu + \frac{\nu_{t0}}{C_\varepsilon}\right)\frac{\partial \varepsilon_0}{\partial x_k} + \frac{\varepsilon_0}{k_i}(C_1 f_0 P - C_2\varepsilon_0). \end{cases} \tag{1}$$

$$P \equiv -\overline{u_{i0}u_{j0}}(\partial U_i/\partial x_j), \quad \nu_{t0} = C_\nu F_\nu k_0^2/\varepsilon_0,$$

$$f_0 = \left(1 - \exp\left(-\frac{\mathrm{Re}_{y0}}{5.5}\right)\right)\left(1 - \exp\left(-2.4\frac{y}{L_{\varepsilon 0}}\right)\right), \tag{2}$$

$$F_\nu = \left(1 - \exp\left(-\frac{\mathrm{Re}_{y0}}{45}\right)\right)\left(1 - \exp\left(-2.4\frac{y}{L_{\varepsilon 0}}\right)\right),$$

$$\mathrm{Re}_{y0} = \sqrt{k_0}y/\nu, \quad L_{\varepsilon 0} = k_0^{3/2}/\varepsilon_0.$$

Test calculations showed that this model allows not only solution of traditional problems but also calculations that are not open to traditional models.

On the basis of these ideas, in [1], model (3) of the type $\overline{t^2} - \varepsilon_t$ for calculation of temperature fluctuations produced in the boundary layer by primary vortices was suggested and tested:

$$\begin{cases} \frac{D\overline{t_0^2}}{D\tau} = f_{0-t}\frac{\partial}{\partial x_k}\left(\alpha + \frac{\alpha_{t0}}{\sigma_t}\right)\frac{\partial \overline{t_0^2}}{\partial x_k} + 2f_{0-t}P_t - 2(\varepsilon_{t0} + \varepsilon_{t0-\mathrm{add}}), \\ \frac{D\varepsilon_{t0}}{D\tau} = f_{0-t}\frac{\partial}{\partial x_k}\left(\alpha + \frac{\alpha_{t0}}{\sigma_{\varepsilon t}}\right)\frac{\partial \varepsilon_{t0}}{\partial x_k} + \frac{\varepsilon_{t0}+\varepsilon_{t0-\mathrm{add}}}{0.5\overline{t_0^2}}(C_{1t}f_{0-t}P_t - C_{2t}\varepsilon_{t0}), \end{cases} \tag{3}$$

$$P_t = -\overline{u_{i0}t_0}\frac{\partial \overline{T}}{\partial x_i}, \quad \overline{u_{i0}t_0} = -\alpha_{t0}\frac{\partial \overline{T}}{\partial x_i}, \quad \alpha_{t0} = C_\lambda F_\lambda k_0 \frac{0.5\overline{t_0^2}}{\varepsilon_{t0} + \varepsilon_{t0-\mathrm{add}}},$$

$$f_{0-t} = \left(1 - \exp\left(-R_0\frac{\mathrm{Re}_{y0}}{5.5}\right)\right)\left(1 - \exp\left(-2.4\frac{y}{L_{\varepsilon 0}}\right)\right), \tag{4}$$

$$F_\lambda = \left(1 - \exp\left(-R_0\frac{\mathrm{Re}_{y0}}{45}\right)\right)\left(1 - \exp\left(-2.4\frac{y}{L_{\varepsilon 0}}\right)\right),$$

$$R_0 = \left(\frac{k_0}{\varepsilon_0}\Big/\frac{0.5\overline{t_0^2}}{\varepsilon_{t0} + \varepsilon_{t0-\mathrm{add}}}\right), \quad \varepsilon_{t-\mathrm{add}} = \max\left(0.5\overline{t^2}\frac{\varepsilon}{k} - \varepsilon_t, 0\right).$$

The present paper gives further development of the ideas suggested.

2. Model of transfer of turbulent stresses

2.1. Model of transfer of turbulent stresses without account for the effect of walls and/or shear

The exact equation of transfer of turbulent stresses is deduced on the basis of the Navier–Stokes equations. It can be written in the form

E-mail address: golovnya@list.ru

0017-9310/$ - see front matter © 2009 Elsevier Ltd. All rights reserved.
doi:10.1016/j.ijheatmasstransfer.2008.07.057

Nomenclature

C_1, C_2, $C\varepsilon$, C_ν constants of the turbulence model
C_f friction coefficient
$C_{fb} = \frac{\nu}{0.5U_b^2}\frac{\partial U}{\partial y}_{y=0}$ stress of frictional forces on the wall
F_ν, f_0 functions of the turbulence model
k total energy of turbulence
k_0, k_1, k_i components of the turbulence energy
L_ε dissipative scale, $k^{3/2}/\varepsilon$
Nu Nusselt number
Re, Re_x Reynolds number, $U_e x/\nu$
Re_y turbulent Reynolds number, $\sqrt{k}y/\nu$
ΔT temperature difference, T_w - T_e
t temperature fluctuation
U, $\overline{U}$ instantaneous and mean velocities in the x direction
$U_b = (g\beta\Delta Tx)^{1/2}$ characteristic velocity of natural convection
u, u_0, u_1, u_i fluctuation components of velocity in the x direction

Greek symbols
δ boundary-layer thickness
ε dissipation rate k, $\nu\overline{(\partial u_i/\partial x_i)^2}$

Subscripts
e in a free flow
w on a wall

$$\frac{D\overline{u_iu_j}}{Dt} = \nu\frac{\partial^2}{\partial x_k\partial x_k}\overline{u_iu_j} + \mathrm{Diff}_{\mathrm{turb}}(\overline{u_iu_j}) + P_{ij} + \pi_{ij} - \varepsilon_{ij}$$

Here $\mathrm{Diff}_{\mathrm{turb}}$ is the operator of turbulent diffusion transfer, P_{ij} is the generation, π_{ij} is the redistribution due to interaction of fluctuations of velocity and pressure, ε_{ij} is the rate of dissipation $\overline{u_iu_j}$.

The values of the generation term are calculated by exact relations:

$$P_{ij} \equiv -\overline{u_iu_k}\frac{\partial U_j}{\partial x_k} - \overline{u_ju_k}\frac{\partial U_i}{\partial x_k} - \beta(g_i\overline{u_jt} + g_j\overline{u_it})$$

Turbulent diffusion, redistribution and dissipation rate must be modeled.

2.2. Equation of transfer of the rate of dissipation ε_{ij}

In the case when $i \neq j$, the correlation $\overline{u_iu_j}$ describes the energy of interaction of the components of the fluctuating component of velocity. This energy cannot be transferred via the cascade process since it originates as a result of interaction of specific fluctuations at a specific instant of time. In [1] it is shown that in the k-ε model constructed on the basis of the suggested ideas ε indicates energy transfer to the cascade process. Hence it follows that in the case $i \neq j$, $\varepsilon_{ij} = 0$. We note that the equality $\varepsilon_{ij} = 0$ follows also from the isotropy of small-scale turbulent motions.

In the case $i = j$, we require that the half-sum of the transfer equations $\overline{u_iu_i}$ coincided with the equation of k transfer. Hence it follows the necessity for the equality $\sum\varepsilon_{ii} = 2\varepsilon$ to be fulfilled. The known relation $\varepsilon_{ii} = 2\varepsilon/3$ satisfies this requirement in full measure but test calculations show that it is better to abandon its use.

In this model, we decided to use a special equation of transfer for calculation of dissipative terms ε_{ii}. This equation is derived from the Navier–Stokes equations and can be written in the form:

$$\frac{D\varepsilon_{ii}}{Dt} = \nu\frac{\partial^2}{\partial x_k\partial x_k}\varepsilon_{ii} + \mathrm{Diff}_{\mathrm{turb}}(\varepsilon_{ii}) + P_{\varepsilon ii} + \pi_{\varepsilon ii} - \varepsilon_{\varepsilon ii},$$

Here $\mathrm{Diff}_{\mathrm{turb}}$ is the operator of turbulent diffusion transfer, $P_{\varepsilon ii}$ is the generation of ε_{ij}, $\pi_{\varepsilon ii}$ is the redistribution of ε_{ij} due to interaction of fluctuations of velocity and pressure, $\varepsilon_{\varepsilon ii}$ is the rate of dissipation of ε_{ij}. All these terms must be modeled.

2.3. Redistribution terms

In this work, the known Rotta [2] relation

$$\pi_{ij} = -C_a\frac{\varepsilon}{k}\left(\overline{u_iu_j} - \frac{2}{3}\delta_{ij}k\right).$$

was used to calculate redistribution.

In constructing the equation of ε_{ij} transfer by the recommendations of Rodi [3] and by analogy with modeling the equations of $\overline{u_i^2}$ and ε transfer, we combine the relations for generation, redistribution, and dissipation as a whole and model as follows:

$$P_{\varepsilon ii} + \pi_{\varepsilon ii} - \varepsilon_{\varepsilon ii} = \frac{\varepsilon}{k}(C_1(P_{ii} + \pi_{ii}) - C_2\varepsilon_{ii})$$

2.4. Turbulent diffusion

Apparently, one of most widely spread models of turbulent diffusion is the gradient model of Daly and Harlow [4]

$$\mathrm{Diff}_{\mathrm{turb}}(\overline{u_iu_j}) = \frac{\partial}{\partial x_k}C_{\mathrm{Diff}}\frac{k}{\varepsilon}\overline{u_ku_n}\frac{\partial\overline{u_iu_j}}{\partial x_n}$$

In this work, this model was used in a slightly simplified form

$$\mathrm{Diff}_{\mathrm{turb}}(\overline{u_iu_j}) = \frac{\partial}{\partial x_k}C_{\mathrm{Diff}}\frac{k}{\varepsilon}\overline{u_k^2}\frac{\partial\overline{u_iu_j}}{\partial x_k} \quad (5)$$

2.5. Account for the effect of the wall and/or shear on the transfer processes

In the k-ε model (1), multiplication of the diffusion terms by the function f_0 is used instead of introduction of additional term into the model, which compensate diffusion on the wall. In the model under development, the near-wall interactions are allowed for in a similar way.

The coefficient of turbulent diffusion $C_{\mathrm{Diff}}\frac{k}{\varepsilon}\overline{u_k^2}$ in (5) is the approximation of a quite particular quantity, presumably proportional eddy viscosity. It is clear that approximation is obtained partially on the basis of experimental data (values of $\overline{u_iu_j}$, $\overline{u_k^2}$, and k), partially on the basis of a immeasurable quantity ε. It is natural to assume that in constructing the approximation the values of ε were found based on one of traditional models. But, assuming the process to be equilibrium, in first approximation we can take that $\varepsilon_{\mathrm{t.m}} \approx f_0\varepsilon_{\mathrm{p.m}}$, where the subscripts t.m and p.m indicate the traditional and present models, respectively. This is well seen from Eq. (1) of the k-ε model. This fact is allowed for in the model for the diffusion term

$$\mathrm{Diff}_{\mathrm{turb}}(\overline{u_{i0}u_{j0}}) = \frac{\partial}{\partial x_k}C_{\mathrm{Diff}}f_0\frac{k_0}{\varepsilon_0}\overline{u_{k0}^2}\frac{\partial\overline{u_{i0}u_{j0}}}{\partial x_k} \quad (6)$$

The model of turbulent diffusion ε_{ii} is constructed by analogy with (6) with account for construction of the equation of dissipation transfer in the k-ε model

$$\mathrm{Diff}_{\mathrm{turb}}(\varepsilon_{i0}) = \frac{\partial}{\partial x_k}\frac{1}{C_\varepsilon}C_{\mathrm{Diff}}f_0\frac{k_0}{\varepsilon_0}\overline{u_{k0}^2}\frac{\partial\varepsilon_{i0}}{\partial x_k}$$

According to the theory stated in [1], as a result of interaction with the wall the energy of turbulence is redistributed over the chain of vortices (primary vortices, secondary vortices, etc.). This process is reflected in the model by multiplication of the generation term by the function f_0. In the model of transfer of turbulent stresses, the generation and redistribution terms take part simultaneously in creation of the energy components $\overline{u_{i0}u_{i0}}$. By virtue of this, we multiply their sum by the function f_0.

In the case when $i \neq j$, the correlation $\overline{u_{i0}u_{j0}}$ describes the energy of interaction of the components of the fluctuating component of velocity. This energy cannot be transferred via the chain of vortices (primary vortices, secondary vortices, etc.) since it appears as a result of interaction of specific fluctuations at a specific instant of time. Therefore, in this case, the generation and redistribution terms must not be multiplied by the function f_0.

The deformation of flow in directed vicinity to the wall is very large and thus pressure fluctuations are also large; in the wall region, the effect of viscous forces remains noticeable, etc. All these reasons cause the wall suppression of the correlation $\overline{u_{i0}u_{j0}}$, which, in turn, requires introduction of an additional term to the equation. The simplest way is to describe this suppression as a part of the generation term, e.g., in the form φP_{ij}, where φ is some function. It is obvious that this function must be related to the distance to the wall. The calculations show that the expression $\varphi = 1 - f_0$ is a good approximation of it.

2.6. Resultant model of transfer of turbulent stresses

After substitution of all approximations and cancellation, the model for calculation of turbulent stresses has the form

$$\begin{cases} \frac{D\overline{u_{i0}^2}}{Dt} = f_0 \frac{\partial}{\partial x_k}(\nu + D_k)\frac{\partial \overline{u_{i0}^2}}{\partial x_k} + f_0\left(P_{ii} - C_a\frac{\varepsilon_0}{k_0}\left(\overline{u_{i0}^2} - \frac{2}{3}k_0\right)\right) - \varepsilon_{i0}, \\ \frac{D\varepsilon_{i0}}{Dt} = f_0 \frac{\partial}{\partial x_k}\left(\nu + \frac{D_k}{C_\varepsilon}\right)\frac{\partial \varepsilon_{i0}}{\partial x_k} + \frac{\varepsilon_0}{k_0}\left(C_1 f_0\left(P_{ii} - C_a\frac{\varepsilon_0}{k_0}\left(\overline{u_{i0}^2} - \frac{2}{3}k_0\right)\right) - C_2\varepsilon_{i0}\right), \\ \frac{D\overline{u_{i0}u_{j0}}}{Dt} = f_0 \frac{\partial}{\partial x_k}(\nu + D_k)\frac{\partial \overline{u_{i0}u_{j0}}}{\partial x_k} + f_0 P_{ij} - C_a\frac{\varepsilon_0}{k_0}\overline{u_{i0}u_{j0}}, \end{cases} \quad (7)$$

Here $D_k = C_{\text{Diff}} f_0 \frac{k_0}{\varepsilon_0}\overline{u_{k0}^2}$, $\quad P_{ij} \equiv -\overline{u_{i0}u_{k0}}\frac{\partial U_j}{\partial x_k} - \overline{u_{j0}u_{k0}}\frac{\partial U_i}{\partial x_k}$.

The values of the constants are: $C_2 = 1.45$, $C_1 = 0.98C_2$, $C_a = 2.8$, $C_{\text{Diff}} = 0.26$, and $C_\varepsilon = 1.3$.

To perform calculations, model (7) is supplemented by model (1) of the k-ε type.

3. Model of transfer of turbulent heat fluxes

3.1. Model of transfer of turbulent heat fluxes without account for the effect of walls and/or shear

The exact equation of transfer of the correlation $\overline{u_i t}$ can be obtained from the Navier–Stokes equations and the equations of transfer of thermal energy. It has the form

$$\frac{D\overline{u_i t}}{Dt} = \text{Diff}_{\text{visc}}(\overline{u_i t}) + \text{Diff}_{\text{turb}}(\overline{u_i t}) + P_{it} + \pi_{it} - \varepsilon_{ir} \quad (8)$$

The following notation is used for the terms: $\text{Diff}_{\text{visc}}$ is the operator of molecular diffusion transfer, $\text{Diff}_{\text{turb}}$ if the operator of turbulent diffusion transfer, P_{it} is the generation, π_{it} is the redistribution, ε_{it} is the rate if dissipation of $\overline{u_i t}$.

The generation is calculated exactly $P_{it} = -\overline{u_i u_j}\frac{\partial T}{\partial x_j} - \overline{u_j t}\frac{\partial U_i}{\partial x_j} - \beta g_i \overline{t^2}$. Assuming that ν and α are the quantities of the same order, for molecular diffusion we can use the relation $\text{Diff}_{\text{visc}}(\overline{u_i t}) = \frac{\nu+\alpha}{2}\frac{\partial^2 \overline{u_i t}}{\partial x_j \partial x_j}$. All the rest terms must be modeled.

3.2. Redistribution terms

To calculate redistribution we used the Monin relation [5]

$$\pi_{it} = -C_{at}\frac{1}{S_{it}}\overline{u_i t}$$

Here S_{it} is the time scale. In the case of transfer of correlation $\overline{u_i t}$ it is calculated as follows.

It is obvious that the lifetime of the correlation $\overline{u_i t}$ is determined by the time of simultaneous existence of temperature and kinematic fluctuations. By this reason, the time scale S_{it} must be determined as $S_{it} = \min(S_{ii}, S_t)$, where S_{ii} is the time scale of $\overline{u_i^2}$, and S_t is the time scale of $\overline{t^2}$. But the time scale of temperature fluctuations cannot be larger than the time scale of kinematic fluctuations. To guarantee this inequality, the author introduced additional dissipation $\varepsilon_{t-add} = \max(0.5\overline{t^2}\frac{\varepsilon}{k} - \varepsilon_t, 0)$ to the equation of $\overline{t^2}$ transfer. It follows from this expression that $\varepsilon_{\text{t-add}}$ is calculated such that fulfillment of the inequality $0.5\overline{t^2}/(\varepsilon_t + \varepsilon_{t-\text{add}}) \leqslant k/\varepsilon$ was guaranteed, i.e., the time scale of temperature fluctuations did not exceed the time scale of kinematic fluctuations. By this reason, the time scale was calculated as

$$S_{it} = \frac{0.5\overline{t^2}}{(\varepsilon_t + \varepsilon_{t-\text{add}})} \quad (9)$$

3.3. Turbulent diffusion

The gradient Launder expression [6]

$$\text{Diff}_{\text{turb}}(\overline{u_i t}) = \frac{\partial}{\partial x_k}\left(C_{\text{Diff}} S_{it}\overline{u_k u_n}\frac{\partial \overline{u_i t}}{\partial x_n}\right)$$

is often used as the model for turbulent diffusion $\overline{u_i t}$. Here S_{it} is the time scale of the process. In the present work, this model was used in a slightly simplified form

$$\text{Diff}_{\text{turb}}(\overline{u_i t}) = \frac{\partial}{\partial x_k}\left(C_{\text{Diff}}\frac{0.5\overline{t^2}}{(\varepsilon_t + \varepsilon_{t-\text{add}})}\overline{u_k^2}\frac{\partial \overline{u_i t}}{\partial x_k}\right) \quad (10)$$

In this case, the choice of the time scale (9) is taken into account.

3.4. Account for the wall effect on transfer processes

In this approach, it is suggested to take into account the effect of walls on transfer by introducing a special function to the equations. By virtue of the consideration formulated when calculating the time scale, as such function we take the function $f_{0\text{-t}}$ of form (4) used in model (3).

The wall effect is taken into account in Eq. (8) in two terms.

First, as in the case of the equations of transfer of $\overline{u_i u_j}$, to allow for the near-wall viscous effects we multiply the diffusion terms by $f_{0\text{-t}}$.

From the considerations given in obtaining the coefficient of turbulent diffusion in the equations of transfer of $\overline{u_{i0}u_{j0}}$, we modify model (10) by multiplying the coefficient of turbulent diffusion by $f_{0\text{-t}}$

$$\text{Diff}_{\text{turb}}(\overline{u_{i0}t_0}) = \frac{\partial}{\partial x_k}\left(C_{\text{Diff}} f_{0-t}\frac{0.5\overline{t_0^2}}{(\varepsilon_{t0} + \varepsilon_{t0-\text{add}})}\overline{u_{k0}^2}\frac{\partial \overline{u_{i0}t_0}}{\partial x_k}\right)$$

Second, as well as in the case of construction of the equation of transfer of the correlation $\overline{u_i u_j}(i \neq j)$, we assume that deformation of turbulent vortices in close vicinity to the wall generates suppression of the correlation $\overline{u_i t}$. As in the equation for $\overline{u_i u_j}(i \neq j)$, we describe this suppression as a part of the generation term related to the distance to the wall. This relation we take into account by the function φ. Test calculations show that the expression $\varphi = 1 - f_{0\text{-t}}$ serves as a satisfactory approximation for it.

As is known, in the case of local isotropy the dissipation $\varepsilon_{it} = (\nu + \alpha)\frac{\partial u_i}{\partial x_j}\frac{\partial t}{\partial x_j}$ is zero, therefore in the present model it is disregarded.

3.5. Resultant model of transfer of turbulent heat fluxes

The resultant model for calculation of turbulent heat fluxes has the form

$$\frac{D\overline{u_{i0}t_0}}{Dt} = f_{0-t}\frac{\partial}{\partial x_k}\left(\frac{\nu+\alpha}{2}+D_{tk}\right)\frac{\partial\overline{u_{i0}t_0}}{\partial x_k} + f_{0-t}P_{it} - C_{at} \times \frac{\varepsilon_{t0}+\varepsilon_{t0-add}}{0.5\overline{t_0^2}}\overline{u_{i0}t_0} \quad (11)$$

Here $D_{tk} = C_{\rm Diff} f_{0-t}\frac{0.5\overline{t_0^2}}{(\varepsilon_{t0}+\varepsilon_{t0-{\rm add}})}\overline{u_{k0}^2}$ is the coefficient of turbulent diffusion in the direction x_k. The constants were chosen from the requirement of the best coincidence of calculations with the experiments and literature data. The final values of the constants are:

$$C_{t2} = 1.45, \quad C_{t1} = 0.9C_{t2}, \quad C_{\rm Diff} = 0.26, \quad C_{\varepsilon t} = 1.3.$$

The constant $C_{\rm at}$ depends on the Pr number. The expression $C_{\rm at} = 2.5 + 0.18{\rm Pr}^{0.73}$ can serve as a reasonable approximation of the dependence in the range $0.7 \leqslant {\rm Pr} \leqslant 50$.

From obvious consideration, the system of Eq. (3) that describes the transfer of $\overline{t_0^2}$ and ε_{t0} must be included to the model.

4. Model testing

4.1. Forced flow in the boundary layer

The model was tested by calculations of forced turbulent convection on a flat plate. The calculations were performed from $Re = 4.0\times10^5$ to 10^8. The coincidence with the experimental data is very good for all parameters. The results of the calculations of friction and heat transfer on the wall are given in Figs. 1 and 2.

4.2. Natural convection on a vertical surface

Calculation of turbulent convection occurring under the effect of Archimedes forces relates to one of very complex problems of turbulent modeling. The available literature data do not allow one to recommend with sufficient accuracy any models for solution of the problems of this class. So, in particular, it follows from the data of systematic analysis [7] of the applicability of the k-ε models to calculation of natural convection that results of calculation are distinguished by a great scatter in both the values of integral parameters and the distributions of such parameters as turbulent energy, eddy viscosity, etc.

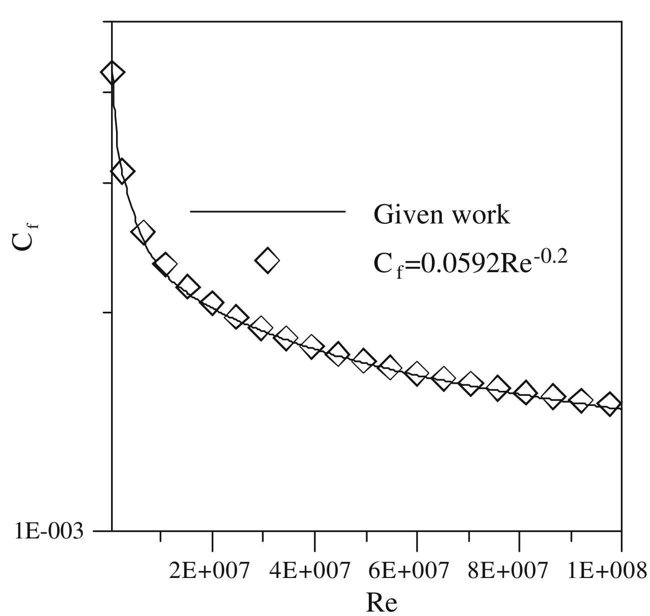

Fig. 1. Turbulent flow in a forced boundary layer. Calculation of the friction coefficient.

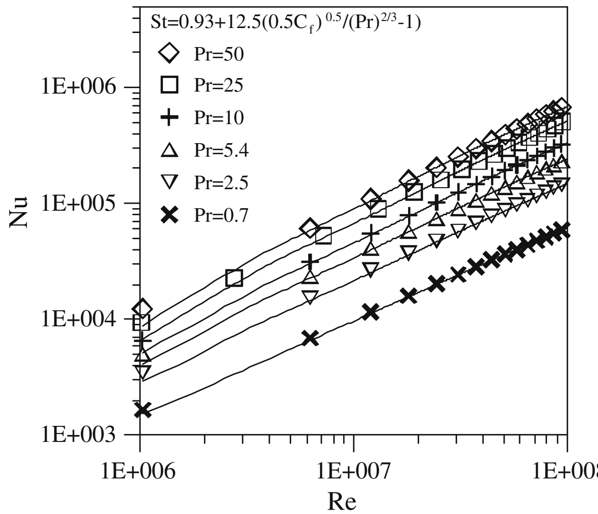

Fig. 2. Turbulent flow in a forced boundary layer. Calculation of heat transfer (solid line) at different Pr numbers.

The suggested model of transfer of turbulent stresses and turbulent heat fluxes was used to calculate natural convection on a vertical plate with $T_{\rm w}$ = const. The calculations were performed from $Gr = 0.8\times10^{10}$ to 10^{13}.

Fig. 3 gives the results of calculation of friction and heat transfer.

Since in natural confection the friction coefficient is meaningless, dimensionless stress of friction forces on the wall $C_{\rm fb}$ was calculated instead of it. In the present work, we compared the results of $C_{\rm fb}$ calculation with the following approximations: (1) Tsuji–Nagano [8], ($C_{\rm fb} = 2{\rm Gr}^{-0.26}$); (2) Cheesewright–Ierokipiotis [9], ($C_{\rm fb} = 1.386{\rm Gr}^{-0.249}$); and (3) Kirdyashkin [10], ($C_{\rm fb} = 20.4{\rm Gr}^{-1/3}{\rm Pr}^{-1/6}$). Calculations of heat transfer were compared with the known formula ${\rm Nu} = 0.12({\rm Gr\,Pr})^{1/3}$.

Results of the calculations of averaged and fluctuating parameters were tested by comparison with the experimental data of Tsuji and Nagano [8]. As is seen from Figs. 4 and 5, agreement is quite satisfactory.

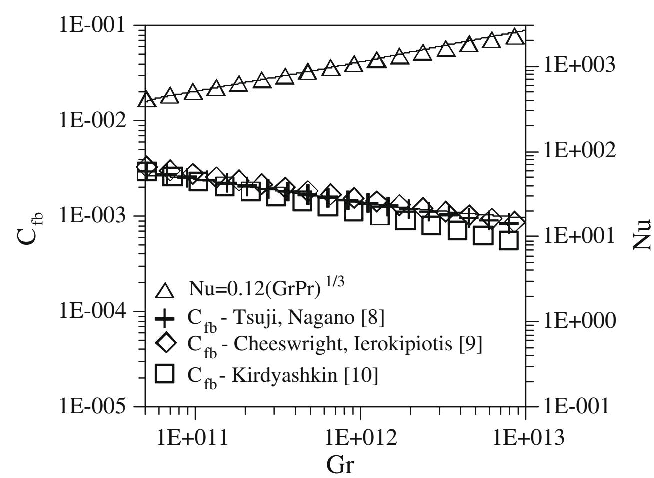

Fig. 3. Friction and heat transfer in natural convection on a vertical surface.

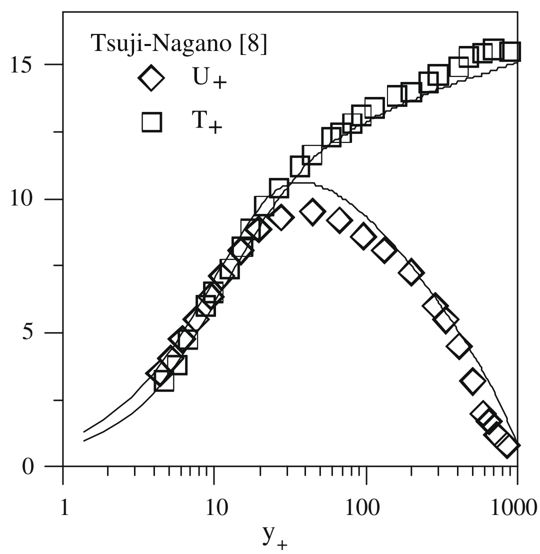

Fig. 4. Turbulent natural convection on a vertical surface. Calculation of average velocity and temperature.

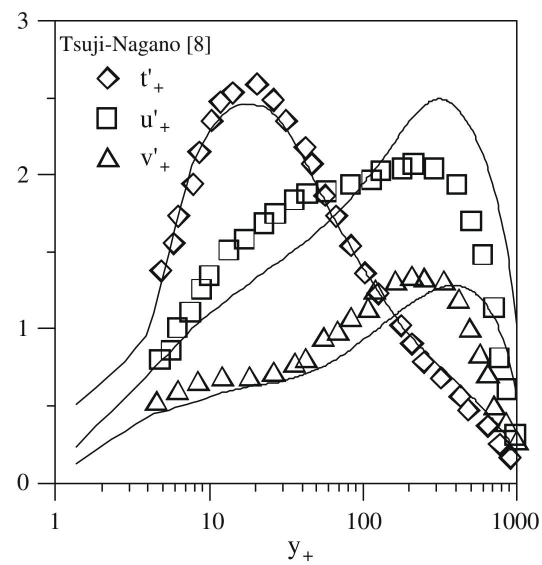

Fig. 5. Turbulent natural convection on a vertical surface. Calculation of fluctuating parameters.

4.3. Flow in channels and tubes

4.3.1. Stabilized flow

The idea used in construction of the model for boundary layer calculation was applied to construction of the model for calculation of flow in channels and tubes. The sense of adaptation is obvious. In the case of the boundary-layer flow, a turbulent vortex is pressed to one wall which is allowed for by the model. In the case of the channel flow, there are two such walls, therefore the both walls must taken into account simultaneously. In other words, the function f_0 for calculation of the channel flow is as follows:

$$f_0 = \left(1 - \exp\left(-\frac{\mathrm{Re}_{1y0}}{5.5}\right)\right)\left(1 - \exp\left(-2.4\frac{H-y}{L_{\varepsilon 0}}\right)\right) \times \left(1 - \exp\left(-\frac{\mathrm{Re}_{2y0}}{5.5}\right)\right)\left(1 - \exp\left(-2.4\frac{H+y}{L_{\varepsilon 0}}\right)\right), \quad (12)$$

$$\mathrm{Re}_{1y0} = \frac{\sqrt{k_0}(H-y)}{\nu}, \quad \mathrm{Re}_{2y0} = \frac{\sqrt{k_0}(H+y)}{\nu}, \quad L_{\varepsilon 0} = \frac{k_0^{3/2}}{\varepsilon_0} \quad (13)$$

Here y is the distance from the channel axis and H is the channel half-width.

For calculation of tube flows, in relations (12) and (13) the distance from the tube center played the role of y and its radius played the role of H.

The results of heat transfer calculation within the range $0.72 \leqslant \mathrm{Pr} \leqslant 50$ in the stabilized tube flow were compared with three known approximations (see [11])

$$\mathrm{Nu}_1 = \mathrm{Re}_D \xi \mathrm{Pr}/(40\sqrt{\xi}(\mathrm{Pr}^{2/3} - 1) + 8), \quad \mathrm{Nu}_2 = 0.023\mathrm{Re}_D^{0.8}\mathrm{Pr}^{0.43},$$
$$\mathrm{Nu}_3 = \mathrm{Re}_D \mathrm{Pr}\sqrt{\xi/2}/(4.24\mathrm{Ln}(\mathrm{Re}_D\sqrt{\xi/16}) + 25\mathrm{Pr}^{2/3} + 4.24\mathrm{Ln}(\mathrm{Pr}) - 20.2).$$

In all cases deviation from one of the formulas did not exceed 3–4%.

Results of the calculations of average and fluctuating parameters demonstrate a very good agreement with the experiments of different authors. As an illustration, Fig. 6 gives calculations of fluctuating components of velocity. We note that calculations of turbulence produced by secondary vortices were not performed.

4.3.2. Stabilizing section

Development of turbulence in tube and channel flows sharply differs by internal regularities from the development of turbulence in a boundary layer. The major difference is that turbulence appears in tubes and channels not due to the instability of laminar profile. In particular, the Poiseuille profile in tube flows is always stable. The main reason of turbulence origination is the presence of disturbances in the flow. But even if the disturbances provide transition to the turbulent mode, there is no guarantee that flow will remain turbulent forever. Upon elapse of a rather large period of time turbulence can degenerate. The dependence of the process of turbulence formation on the structure of disturbances is very complex and has not been adequately studied. Darbyshire and Mullin [12] and Hof et al. [13] note that experiments in short tubes, i.e., in tubes with a length of about 100D cannot reproduce the entire picture of turbulence formation. To obtain the whole patter we require longer tubes and a much larger period of observation.

The process of turbulent flow stabilization in a tube inherently is the process of the development of disturbances in an incoming flow. It follows from the said above that we can require full coincidence of the calculated and experimental data only if the structure of the incoming flow is absolutely known. In the present work, all

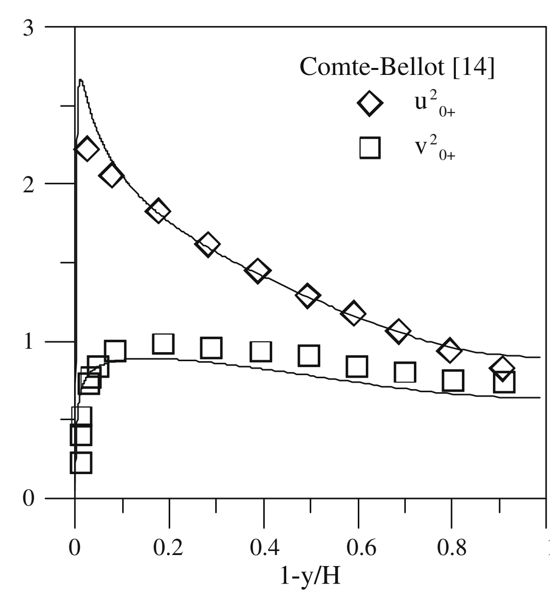

Fig. 6. Turbulent channel flow. Calculation of fluctuating components of velocity.

calculations were conducted starting from the rectangular profiles of average velocity, energy of turbulence, and dissipative scale, which, most likely, does not correspond to the conditions of the experiment. We note that the rate of dissipation and dissipative scale do not refer to the measured parameters of the flow. We consider some results of calculations.

Fig. 7 shows the dynamics of variation of the mean dissipative scale in channel flow. Here the mean scale was calculated as $L_{\text{mid}} = \frac{1}{2H}\int_{-H}^{H} L_\varepsilon(y)dy$. It is well seen from the figure that a flow with small scales of vortices at the channel inlet is stabilized most quickly. A minimum length of the stabilizing section is of about 300*H*. The stabilizing section noticeably increases with an increase of the scale. If we consider the rectangular profile at the channel inlet as the stabilized profile plus the disturbance imposed on it, then the process of stabilization can be treated as the process of decay of disturbances. The results presented indicate that the stronger the disturbance the more is the period of its decay. This conclusion is in good qualitative agreement with the data of [12,13].

On the other hand, by the data of Comte-Bellot [14] the channel flow was stabilized on the section 120*H*, where *H* is the channel half-width. The results of calculations show that in the calculations we restrict ourselves only to this channel length, then we can take the flow to be stabilized if the dissipative scale of the incoming flow is more that 0.3*H*.

The author calculated the friction coefficient in the initial section of the tube for dissipative scales of the incoming flow, which vary within the range from 0.5*H* to 0.9*H*. The results were compared with calculations by four known formulas:

$$\xi_1 = 0.0032 + 0.22\text{Re}_D^{-0.237}, \quad \xi_2 = 1/(0.78\text{Ln}(\text{Re}_D) + 1.64),$$
$$\xi_3 = 0.3164/\text{Re}_D^{0.25}, \quad 1/\sqrt{\xi_4} = 0.87\text{Ln}(\text{Re}_D\sqrt{\xi_4}) - 0.41.$$

In all cases, results of calculations at *X* = 120*H* are in quire reasonable agreement with calculations by one of the given formulas. We note that scatter of the friction coefficients calculated by these formulas turns to be higher than variation of the friction coefficient depending on the initial scales.

It should also be noted that values of mean fluctuating parameters cal also be considered stabilized if we restrict ourselves to the channel length 120*H*. As an example we give the results of calculations of turbulent heat fluxes and turbulent friction (see Fig. 8). They, within the limit of the experiment, can also be taken stabilized.

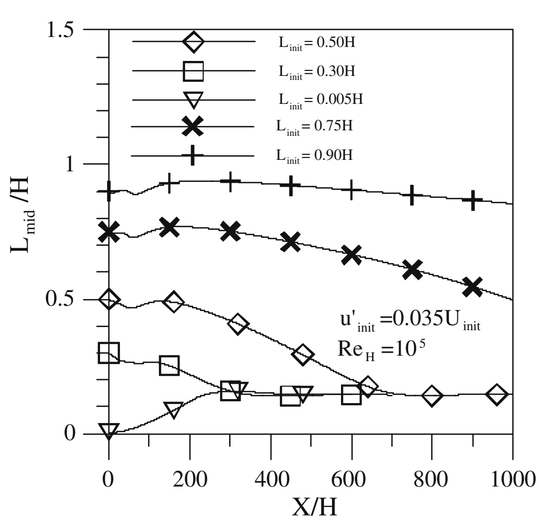

Fig. 7. Dynamics of variation of a mean dissipative scale in a channel flow.

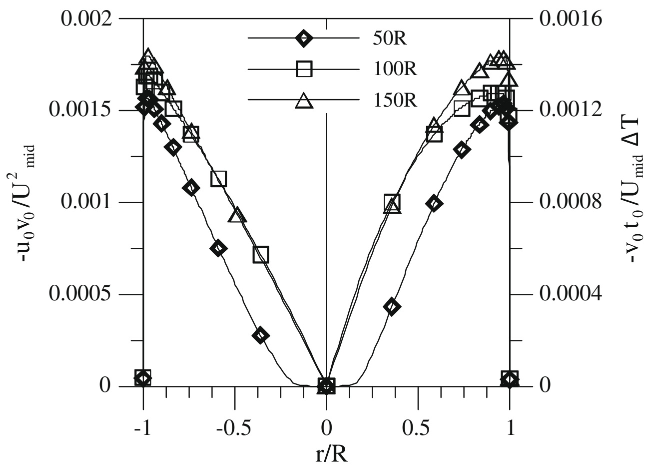

Fig. 8. Calculation of turbulent friction and turbulent heat fluxes at different distance from the tube inlet.

By virtue of said there arises the question: which dissipative scale should be taken as initial data in order to obtain calculations adequate to experimental data. Calculations of pressure, profiles of average velocity and temperature in tubes and channels show that the best agreement with the experimental data is obtained at $L_{\varepsilon\text{-init}} \approx 0.9H$.

At the same time we should emphasize that if at noticeable distances from the channel/tube inlet the effect of the dissipative scale of the incoming flow on fluctuating characteristics turns to be weak, then at small distances it must not be neglected no way. This is demonstrated by calculations given in Fig. 9. The figure shows the dependence of basic fluctuating parameters of the flow on the dissipative scale of the incoming flow at a distance *X* = 5*H*. As is well seen, the dependence is very pronounced. Especially strong is the effect of the dissipative scale on the energy of turbulence.

4.4. Flow past backward-facing step

Turbulent flow past backward-facing step is a widely used test problem for estimating the turbulence models. It is known that errors of the standard *k*-ε model with the wall functions in calculating the coordinate of flow reattachment past the backward-facing step is of about 20–25%.

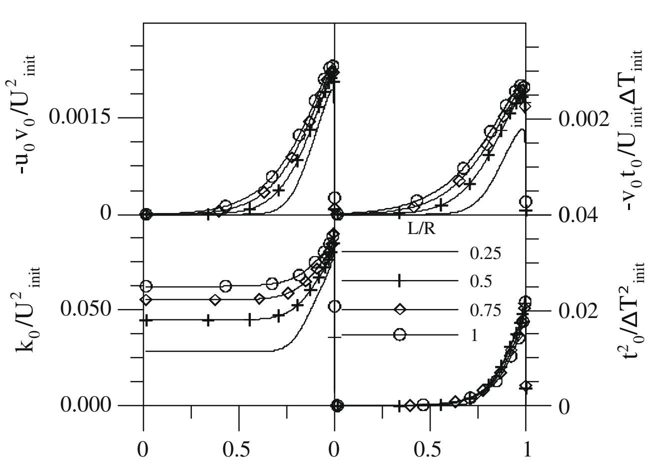

Fig. 9. Dependence of turbulent pipe flow on dissipative scales of an incoming flow. Initial section of flow.

We now present some examples of calculations. So et al. [15] give results of calculation of turbulent flow past a backward-facing step, which was experimentally studied by Eaton and Johnston in [16], by several model of turbulence. In [17], the results of calculation of flow that was studied by Driver and Seegmiller [18] experimentally are compared with calculations by the models of Launder and Sharma [19] and Wilcox [20]. The site NPARC Alliance [21] gives the comparison of the calculations of turbulent flow past the backward-facing step by three turbulence models of the k-ε type (the authors of the models are not indicated) and by the SST model [22] with the experimental data of Driver and Seegmiller [18]. Papageorgakis and Assanis [23] give the calculations of flow past the backward-facing step, which was studied experimentally by Kim et al. [24], by the linear and nonlinear models of Yakhot and Orzsag [25].

Results of the calculation of the point of flow reattachment are given in Table 1. The table presents the models of the mixing length type (model 2), k-ε-type models using the Boussinesq hypothesis (models 1, 3, 5, 7, and 8), the model that uses ε as a dissipative variable but not uses the Boussinesq hypothesis (model 4), two models (7) and (8) that use, at least in the wall region, the turbulence frequency ω as the dissipative variable, and two models of the RNG type.

Generally speaking, the results presented in the table are poorly tractable. For example, declining the Boussinesq hypothesis (calculation 4) gave a worse result than calculations by the models using the Boussinesq hypothesis (calculations 1, 5, 7, and 8). The RNG model with nonlinear terms (calculation 11) shows worse results than the linear RNG model (calculation (10), etc.

In the author's opinion this senselessness can be explained as follows. In Section 4.3.1 we discussed a noticeable dependence of the calculations of the initial section of flow on the dissipative scale at the tube/channel inlet. In the case of flow past a backward-facing step, the conditions behind the step can be treated as calculation of flow in the channel initial section. It is meant that in the experiments of Eaton and Johnston [16] and Kim et al. [24], which were used as a test problem in all calculations except 6–9, the length of the section in front of expansion is equal to about 2.5–3 of the height of the narrow part of the channel. Then it is clear that the dissipative scale at the inlet can rather strongly change the results of calculations. At the same time, none of the works indicate either the dissipative scale or dissipation.

Table 1
Results of calculation of the point of flow reattachment by different models of turbulence.

No.	Model	Deviations from the experiment (%)
1	Chien [26]	−23
2	Rotta [27]	−24
3	Gibson and Younis [28]	−36
4	Launder, Reece, and Rodi [29]	−36.5
5	Launder and Sharma [19]	−16
6	Wilcox [20]	+3
7	Standard k-ε	−15
8	k-ε with the variable C_μ	−11
9	Menter [22]	+2.7
10	Linear RNG [25]	+9
11	Non-linear RNG [25]	+19

A strange behavior of the RNG models is also explained by a scale incorrectly specified at the inlet. Most likely, the dissipation at the channel inlet specified in the calculations is noticeably elevated. In this case, the flow near the lower wall is noticeably laminarized and the reattachment point is shifted away. By increasing the dissipation we can substantially decrease the coordinate of the reattachment point. Then, the reattachment point obtained by the nonlinear model will be closer to the experimental data than the point found by the linear model.

The success of the Menter model [22], which uses $\omega = k^{0.5}L_\varepsilon$, as the dissipative variable in the near-wall region, and the Wilcox model [20], which uses ω as the dissipative variable within the entire computational region is not explained by new dissipative variable only. In these calculations, the problem that was experimentally studied by Driver and Seegmiller [18] was solved. In contrast to experimental works of Kim et al. [24] and Eaton and Johnston [16], where the ratio of the step height to the channel height was 1:3, in [10] this ratio was 1:9. Thus, the flow in the detachment region becomes much closer to the flow unbounded from above. In other words, the flow, in essence, turns to be a boundary layer incoming on the step. But in this case, as is shown by author's calculations, the dependence of the flow on the initial dissipative scales is less pronounced. Hence we can draw a conclusion that only calculations 6–9, which used for comparison the data of [18], have an objective characteristic of the properties of models.

Unfortunately, calculation of flow [18] requires computational power which is not accessible to the author. By virtue of this, in the present paper, we calculated a turbulent flow past a backward-facing step, which was experimentally studied by Kim et al. [24]. The sketch of the computational region is given in Fig. 10.

The ratio of the step height to the channel height at the inlet is 1:3; the Reynolds number calculated by the step height and the mass-mean flow velocity is Re = 44,000.

The independence of the solution on the grid in zone 2 was verified by calculations on two uniform grids: 120 × 62 and 165 × 80. The difference in calculations of the reattachment point is of about 2–3%. At the same time, by the data of Thangam and Speziale [30] the resolution 166 × 73 is sufficient.

The data of Kim et al. [24] are not enough for conducting calculations adequate to the experiment. The published data do not allow one to find the level of fluctuations and the dissipative scale at the setup inlet. Due to this fact, additional studies were needed before calculations.

It is seen from the conditions at the inlet to zone 1 that at the given Re number the flow is defined by two parameters—$u_{\text{inlet}}/U_{\text{inlet}}$ and $L_{\varepsilon\text{-inlet}}/H$, i.e., fluctuations and the dissipative scale at the channel inlet. Fig. 11 shows the results of calculations of the reattachment point as a function of $u_{\text{inlet}}/U_{\text{inlet}}$ and $L_{\varepsilon\text{-inlet}}/H$. The experimental reattachment point $X_{\text{Reatt}}/H = 7$ is shown by the bold line.

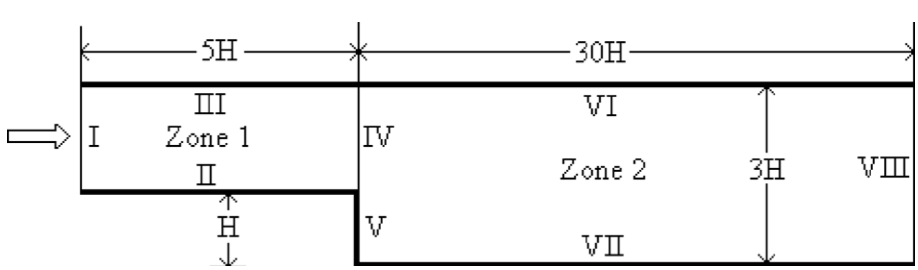

Fig. 10. Flow past a backward-facing step. Sketch of the computational domain.

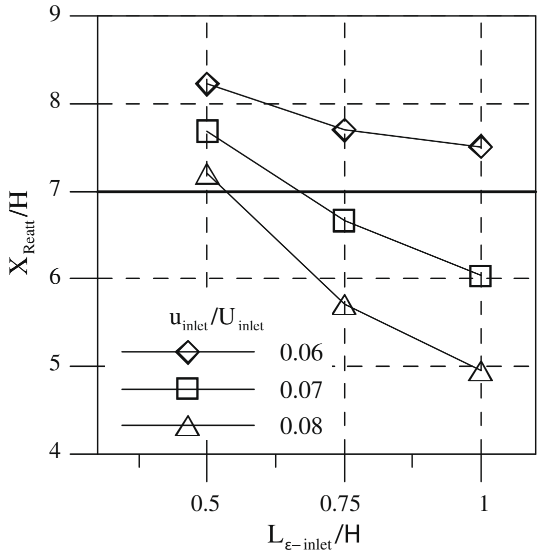

Fig. 11. Flow past a backward-facing step. Dependence of the point of flow reattachment on dissipative scales and the level of fluctuations at the entrance to the computational domain (conditions on boundary I).

The results in Fig. 11 are interpreted trivially. As the level of fluctuations at the inlet decreases the turbulence in the flow decreases and the flow approaches, by the characteristics, the laminar wall jet. In this case, the reattachment point is determined by natural expansion of the jet and, as a result, is shifted downflow. Since $L_\varepsilon = k^{3/2}/\varepsilon$, the increase of the initial dissipative scales is equivalent to initial dissipation decrease. As a result, the level of fluctuations decreases sharply and we obtain a similar picture.

To compare with the experimental data we conducted calculations of flow with the determining parameters $u_{\text{inlet}} = 0.06363U_{\text{inlet}}$ and $L_{\varepsilon\text{-inlet}} = H$. These values were found by interpolation of the data presented in Fig. 11. The calculation coordinate of the reattachment point $X_{\text{Reatt}} = 6.998H$. Allowing for the fact that in [24] $X_{\text{Reatt}}/H = 7 \pm 1$, we have virtually exact coincidence with the experiment.

At the same time, the ambiguity of the solution which satisfies the requirement $X_{\text{Reatt}}/H = 7$ clearly follows from Fig. 11. Thus, there is no much sense in requiring the coincidence of calculation with the experiment. Moreover, we note that in calculations only the equations for primary vortices were used. Hence it follows the underestimation of the calculated values of $\overline{u_0^2}$ compared with the experimental data.

Fig. 12 gives the calculation of the average velocity distribution. The experimental data are shown by symbols. With account for the comments given the agreement is rather satisfactory.

5. Versatility of approach

In the present paper, we assume, by analogy with a laminar flow, that the following physical effect is present in turbulent flows—an additional turbulent vortex appears in the flow as a result of the contact between the turbulent vortex and the surface and/or shear region. The account of this effect in turbulence modeling allows obtaining of very simple and rather universal models of turbulence. But all models suggested in the present work use the variable ε as the dissipative variable. In this section it is shown that transfer of the suggested regularities on the models of turbulence with other dissipative variables allows obtaining of the results of the same quality. The presented calculations are performed on the basis of the k-ω and k-L models, but, as follows from calculations, this technique can elementary be transferred to any other models.

5.1. Technique for constructing turbulence models with arbitrary dissipative variables

According to Launder [31], the dissipative variable z of any model of two differential equations can be presented in the form $z = k^n L^m$, where k is the turbulence energy and L is the dissipative scale. Hence it follows that any two dissipative variables z and z_1 can be related by the expression $z_1 = k^n z^m$. In the present paper, this relation is used for transition from one dissipative variable to another.

We assume that $\varepsilon_0 = k_0^n z_0^m$, where z is a new dissipative variable, and substitute this expression to the equation of dissipation transfer of model (2). After simple transformations we obtain

$$U_i \frac{\partial z_0}{\partial x_i} = f_0 \frac{\partial}{\partial x_i} D_\varepsilon \frac{\partial z_0}{\partial x_i} + \frac{z_0}{k_0}\left[\left(\frac{C_1 - n}{m}\right) f_0 P - \left(\frac{C_2 - n}{m}\right) k_0^n z_0^m\right] + \text{Add} \tag{14}$$

Eq. (14), by its structure, principally corresponds to the equation of dissipation transfer of model (2). The term Add in (14) describes additional terms arising due to the substitution of the dissipative variable.

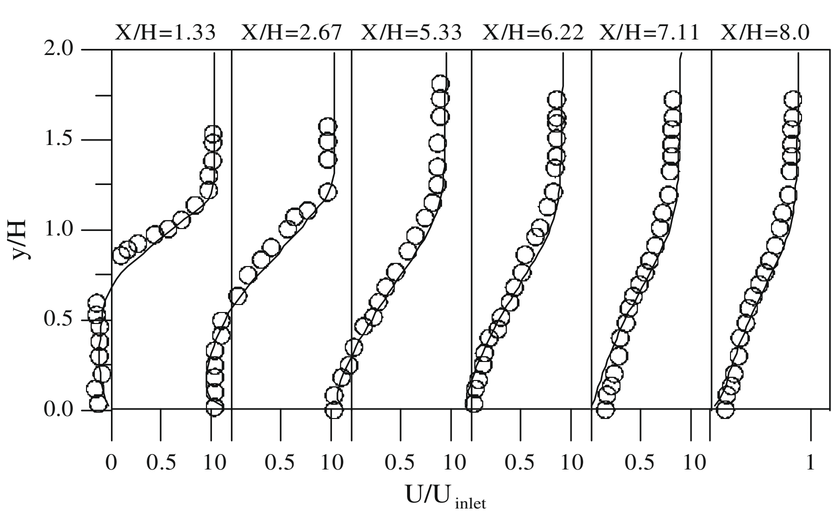

Fig. 12. Flow past a backward-facing step. Distribution of the longitudinal velocity. Symbols – experiment.

In particular, $\varepsilon = k\omega$ for the k-ω model, i.e., $n = m = 1$. Hence

$$U_i \frac{\partial \omega_0}{\partial x_i} = f_0 \frac{\partial}{\partial x_i} D_\varepsilon \frac{\partial \omega_0}{\partial x_i} + \frac{\omega_0}{k_0}[(C_1 - 1) f_0 P - (C_2 - 1) k_0 \omega_0] + \mathrm{Add}_\omega.$$

The term Add_ω has the form

$$\mathrm{Add}_\omega = 2 f_0 D_\varepsilon \frac{1}{k_0} \frac{\partial k_0}{\partial x_i} \frac{\partial \omega_0}{\partial x_i} + \frac{\omega_0}{k_0} f_0 \frac{\partial}{\partial x_i}(D_\varepsilon - D_k) \frac{\partial k_0}{\partial x_i}$$

For the k-L model $\varepsilon = k^{3/2}/L$, i.e., $n = 3/2$, $m = -1$. Hence

$$U_i \frac{\partial L_0}{\partial x_i} = f_0 \frac{\partial}{\partial x_i} D_\varepsilon \frac{\partial L_0}{\partial x_i} + \frac{L_0}{k_0}\left[\left(\frac{3}{2} - C_1\right) f_0 P - \left(\frac{3}{2} - C_2\right) \frac{k_0^{3/2}}{L_0}\right] + \mathrm{Add}_L.$$

The term ADD_L is not used in what follows and therefore is not given here.

After discarding additional terms we obtain two models: the k-ω model (15)–(17)

$$U_i \frac{\partial k_0}{\partial x_i} = f_0 \frac{\partial}{\partial x_i} D_k \frac{\partial k_0}{\partial x_i} + f_0 P - k_0 \omega_0, \tag{15}$$

$$U_i \frac{\partial \omega_0}{\partial x_i} = f_0 \frac{\partial}{\partial x_i} D_\varepsilon \frac{\partial \omega_0}{\partial x_i} + \frac{\omega_0}{k_0}(f_0 (C_1 - 1) P - (C_2 - 1) k_0 \omega_0), \tag{16}$$

$$\nu_t = C_\nu F_\nu k_0 / \omega_0, \tag{17}$$

and the k-L model (18)–(20)

$$U_i \frac{\partial k_0}{\partial x_i} = f_0 \frac{\partial}{\partial x_i} D_k \frac{\partial k_0}{\partial x_i} + f_0 P - \frac{k_0^{3/2}}{L_0}, \tag{18}$$

$$U_i \frac{\partial L_0}{\partial x_i} = f_0 \frac{\partial}{\partial x_i} D_\varepsilon \frac{\partial L_0}{\partial x_i} + \frac{L_0}{k_0}\left(f_0\left(\frac{3}{2} - C_1\right) P - \left(\frac{3}{2} - C_2\right) \frac{k_0^{3/2}}{L_0}\right), \tag{19}$$

$$\nu_t = C_\nu F_\nu \sqrt{k_0} L_0. \tag{20}$$

In the original k-ω model of Wilcox [20] the dissipative term in the equation of k transfer is written as $Ck\omega$, where $C = 0.09$ which allowed one to get rid of the constant $C_\nu = 0.09$ in expression (17). But, as obviously follows from the system (15)–(17), if we introduce the variable $\omega_1 = 0.09\omega$, we can, by changing only the set of constants, remain the previous solution of the system. By this reason, this constant in the given model is taken to be unity.

5.2. Boundary conditions on the wall

For the k-ε model, the boundary condition on the wall were specified in an ordinary manner $y = 0 - U = k = \varepsilon = 0$.

The problem with the boundary condition for ω_0 on the wall requires additional studies. An analysis of the equations of transfer (15) and (16) shows that on the wall they can be written as

$$f_0 \nu \frac{\partial^2 k_0}{\partial y^2} = k_0 \omega_0, \tag{21}$$

$$f_0 \nu \frac{\partial^2 \omega_0}{\partial y^2} = (C_2 - 1)\omega_0^2. \tag{22}$$

In the near-wall region the values of Re_{y0} and $y/L_{\varepsilon 0}$ are small. Therefore, allowing for the expansion of the exponent into the Taylor series, the expression for f_0 can be written in the following form

$$f_0 \approx \frac{\mathrm{Re}_{y0}}{5.5} \frac{2.4y}{L_{\varepsilon 0}} = \frac{1}{5.5} \frac{\sqrt{k_0} y}{\nu} 2.4y \frac{\varepsilon_0}{k_0^{3/2}} \approx 0.44 \frac{y^2 \varepsilon_0}{k_0 \nu} = 0.44 \frac{y^2 \omega_0}{\nu}$$

Then Eq. (21) can be written as

$$0.44 y^2 \frac{\partial^2 k_0}{\partial y^2} = k_0 \tag{23}$$

Eq. (23) has an exact solution

$$k_0 = C_1 y^{\frac{1+\sqrt{10.1}}{2}} + C_2 y^{\frac{1-\sqrt{10.1}}{2}} \approx C_1 y^{2.088} + C_2 y^{-1.088} \tag{24}$$

Since $k_{\mathrm{wall}} = 0$, $C_2 = 0$ and we have the solution $k_0 = C_1 y^{2.088}$ which is in good agreement with the known solutions and experimental data.

By analogy with (23) we write Eq. (22) in the form

$$\frac{0.44}{C_2 - 1} y^2 \frac{\partial^2 \omega_0}{\partial y^2} = \omega_0. \tag{25}$$

Allowing for the fact that in this model $C_2 = 1.45$ and assuming $0.44/0.45 \approx 1$ we find an approximate form of the general solution of Eq. (25)

$$\omega_0 = C_1 y^{(1+\sqrt{5})/2} + C_2 y^{(1-\sqrt{5})/2} \approx C_1 y^{1.62} + C_2 y^{-0.62}.$$

We require that the dissipative scale on the wall was zero. This is quite an obvious requirement since the vortex with zero energy must have a zero diameter. Allowing for (24) we have that if $C_2 = 0$, then $L_{\varepsilon 0} = \sqrt{k_0}/\omega_0 = C_L y^{-0.58}$, i.e., $L_{\mathrm{wall}} = \infty$. Hence it follows that $C_2 \neq 0$ and $\omega_{\mathrm{wall}} = \infty$. In other words, in the calculations the boundary condition $\omega_{\mathrm{wall}} = \infty$ must be approximated, which is rather difficult. These reasons likely cause the necessity in the k-ω model of Wilcox [20] to specify rather a large value of ω on the wall. We note that in this case we obtain on the wall $L_{\varepsilon 0} = \sqrt{k_0}/\omega_0 = C_L y^{1.66}$.

On the other hand, from the considerations of dimensionality $\tau \approx \omega^{-1}$, where τ is the time scale of turbulence. It is evident that in turbulence decay, e.g., when approaching the wall, one of the scales must tend to zero, since in the degenerated turbulence none of the characteristics can have nonzero finite values. The calculations show that in the k-ε model the turbulence frequency, i.e., ω, tends to zero. The above analysis shows that to meet the condition $L_{\mathrm{wall}} = 0$ the k-ω model requires the time scale to tend to zero. As a result, the boundary condition for ω on the wall was selected such that the dissipative scale had minimum correspondence to the dissipative scale that is obtained in the calculations by the k-ε model. The calculations show that in the boundary layer the value $\omega_{\mathrm{wall}} = 500$ corresponds more or less to this condition.

We note one very important fact. It is clear that in the near-wall region the dominant role is played by viscous diffusion which is determined by the second derivative in the direction normal to the wall. Hence it follows that in constructing the difference analogue of the transfer equation ω in the near-wall region, one should, first of all, take care of the accuracy of reproduction of this derivative. As has been already mentioned, the boundary condition $\omega_{\mathrm{wall}} = \infty$ must be specified in the calculations. We assume that on the wall ω is described by the expression $\omega = C/y^n$. Requiring the coincidence of the difference derivative $\omega''_{y1} = (\omega_2 - 2\omega_1 + \omega_{wall})/h^2$ with the exact value, we obtain $\omega_{wall} = (n(n+1) - 2^{-n} + 2)C/h^n$. Hence it follows that in the calculations ω_{wall} is not constant but depends on the grid steps in the direction normal to the wall.

In calculations by the k-L model the boundary condition $L_{\mathrm{wall}} = 0$ was used on the wall. No problem arose when this condition was used.

5.3. Results of calculation of boundary-layer flows

It is obvious that calculations of the boundary layer appreciably depend on the initial conditions. Among the models under consideration the most tested one is the k-ε model. At the same time, the author has not tested the k-ω and k-L models within the framework of the given approach. Therefore, in calculations by the k-ω and k-L models the initial conditions were specified as follows. All calculations were started by the k-ε model at $\mathrm{Re} = 5.0 \times 10^5$. If testing by the k-ω and k-L models was assumed, then at $\mathrm{Re} = 7.0 \times 10^5$ calculation was switched over to the corresponding model equation with the values found by the k-ε model being used as the initial conditions for L or ω.

At the infinity, the condition $\omega_e = 0$ was used in the calculations by the k-ω model.

Results of the calculations by the k-ω model show one more difficulty. In calculations by the k-ω model, a naked sharp increase of the dissipative scale appears on the outer boundary. The rise starts behind the boundary layer border, i.e., where $\partial U/\partial y = 0$, gradually spreads over the entire layer, and appreciably distorts the results of calculations. Change of boundary conditions on the outer boundary did not helped in eliminating this phenomenon.

Probably, Menter [22] implied this very fact when he spoke about formulation of boundary conditions on the outer boundary. To improve the situation, in [22] it was suggested to introduce a correction term, which, on the outer boundary, converts the equation of ω transfer to the equation of ε transfer. To do this, an additional term was introduced to the equation of ω transfer, which by sense was similar to the additional term Add_ω in Eq. (5). This additional term was multiplied by the function that is equal to zero on the wall and to unity on the outer boundary of the layer, so the correction was fully used only on outer boundary of the flow. We note that in [22] the correction is introduced not quite correctly. In [22], it looks like $2\sigma_\varepsilon v_t \frac{1}{k}\frac{\partial k}{\partial x_i}\frac{\partial \omega}{\partial x_i}$. Here the coefficients of diffusion transfer $D_k = v + v_t$ and $D_\omega = v + \sigma_\omega v_t$ are used. Then, since $D_k \neq D_\omega$, a term $\frac{\omega}{k}\frac{\partial}{\partial x_i}(D_\omega - D_k)\frac{\partial k}{\partial x_i}$, as it follows from the above-given conclusion, must be present in the correction. At the same time, viscous diffusion is ignored in the correction. It is natural that inside the layer it can be neglected, but beyond the edge of the boundary layer it may exert appreciable effect.

In order to transform one equation to another Menter [22] used a very complex function of k and ω. Due to the presence of the function f_0 in the model, the values of ω obtained by the Menter [22] model and the studied model will differ greatly. Therefore, direct use of the suggested transformation function is impossible. At the same time, the main meaning of this function is in the fact that it is equal to zero on the wall and to unity on the outer boundary of the layer. The calculations show that the graph of the function f_0^8 and the graph of the function F_1, which was suggested by Menter, are in good coincidence in the boundary layer.

In what follows, we call the model

$$U_i\frac{\partial k_0}{\partial x_i} = f_0\frac{\partial}{\partial x_i}(v+v_t)\frac{\partial k_0}{\partial x_i} + f_0 P - k_0\omega_0,$$

$$U_i\frac{\partial \omega_0}{\partial x_i} = f_0\frac{\partial}{\partial x_i}(v+v_t)\frac{\partial \omega_0}{\partial x_i} + \frac{\omega_0}{k_0}[(C_1-1)f_0P - (C_2-1)k_0\omega_0] + f_0^8\left(2f_0(v+v_t)\frac{1}{k_0}\frac{\partial k_0}{\partial x_i}\frac{\partial \omega_0}{\partial x_i}\right).$$

as the k-ω model with the Menter correction. By virtue of the difficulties mentioned, this model was used in the calculations of the boundary layer instead of the k-ω model suggested by Wilcox [20].

The calculations presented were performed without any optimization of the models. It should be mentioned that in many cases the agreement of calculations by the three models turns to be so good that the graphs virtually merge and are indiscernible.

5.3.1. Boundary-layer flow on the flat surface with the zero pressure gradient and zero turbulence of the outer flow

In these calculations, in the equations of the k-L model the constant $C_{L1} = 1.5\text{-}0.9C_2$ was used, whereas in the k-ε model use was made of the constant $C_1 = 0.93C_2$. No other changes were made. Fig. 13 shows the calculation of the friction coefficient. It is well seen from the graphs that calculations by the k-ε model and the k-ω model with the Menter correction coincide fairly well. A similar qualitative agreement between the calculations is observed in the calculations of all averaged and fluctuating parameters of the flow. The k-L model gives some difference in the obtained values of energy and turbulent friction in the outer region.

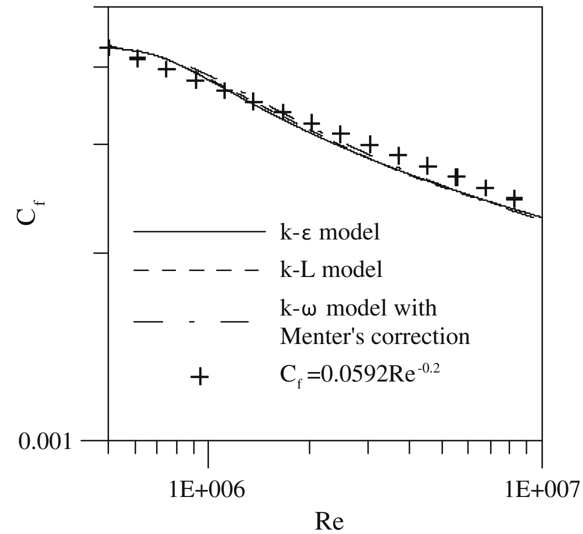

Fig. 13. Turbulent boundary layer. Calculation of the friction coefficient by three turbulence models.

5.3.2. Boundary layer with a positive pressure gradient

The results of calculation of the friction coefficient are presented in Fig. 14. They are compared with the experimental data of Samuel and Joubert [32]. In this case, calculations by the k-ε model and the k-ω model with the Menter correction are in good agreement as well. The k-L model gives some difference in the obtained values of energy and turbulent friction.

5.3.3. Bypass transition in the boundary layer

The technique of calculations is described in [1]. The results of calculations of the friction coefficient are given in Fig. 15. These results are compared with the experimental data of T3A and T3B presented by Roach and Brierly in [33]. We note that coincidence of the calculations of averaged and turbulent parameters with LES calculations of Yang and Voke [34] not worse but sometimes better agreement with the experiment.

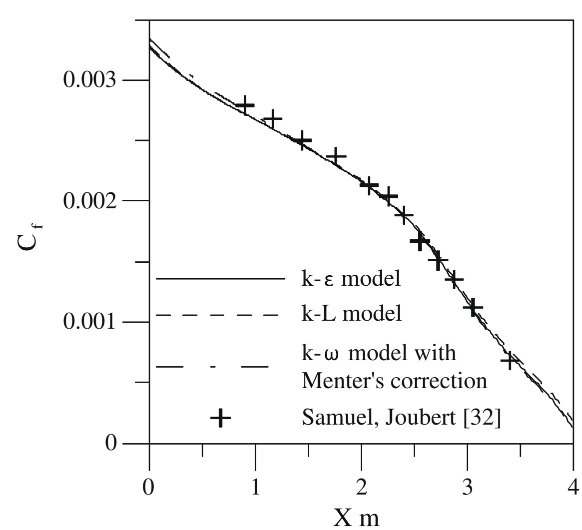

Fig. 14. Flow with a positive pressure gradient. Calculation of the friction coefficient by three turbulence models.

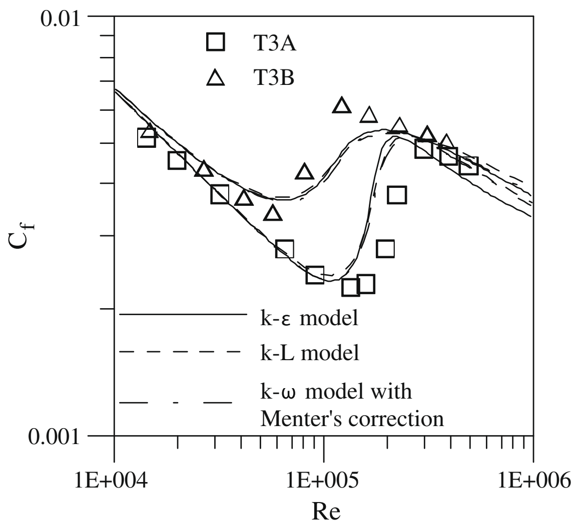

Fig. 15. Bypass transition in the boundary layer. Calculation of the friction coefficient by three turbulence models.

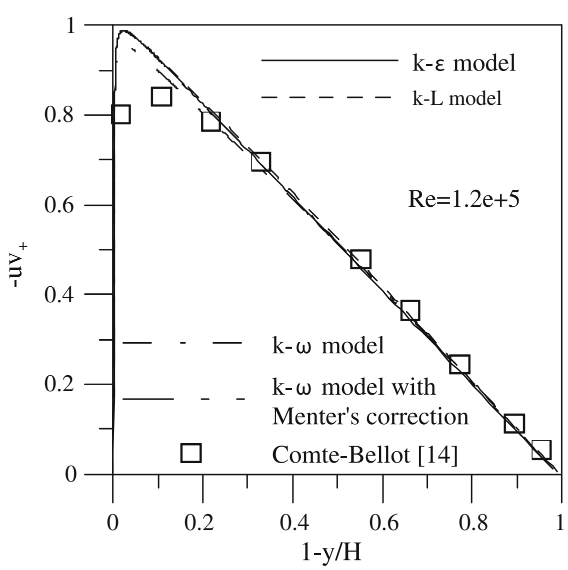

Fig. 16. Flow in a flat channel. Calculation of turbulent friction by three turbulence models.

5.4. Channel flow

Fig. 16 shows the calculations of turbulent friction in stabilized flow in a flat channel. The results are compared with the experimental data of Comte-Bellot [14]. In this case, the use of the Menter correction does not substantially affect the result.

5.5. Additional notes

It is impossible to make direct comparison of calculations of elliptic flows by the model of transfer of turbulent stresses and heat fluxes. The reason is that it is not clear how can the model of transfer of turbulent stresses and heat fluxes be constructed on the basis of *k*-ω and *k*-*L* variables. In the *k*-ε model, the dissipative variable is the energy transferred to the cascade process. Since $k_0 = 0.5(u_0^2 + v_0^2 + w_0^2)$, it is quite natural to assume that $\varepsilon_0 = 0.5(\varepsilon_{u0} + \varepsilon_{v0} + \varepsilon_{w0})$. But this assumption does not cover either the scale of turbulence or its frequency. It should be noted that this limitation appreciably narrows the possibilities of further development of the *k*-ω and *k*-*L* models.

6. Conclusions

In the present paper, the model of transfer of turbulent stresses and heat fluxes is constructed on the basis of the ideas suggested by the author. The verification of the model shows its high efficiency. At the same time, equations of the model are rather simple and involve a minimum number of corrections. One, nevertheless, must pay attention to the fact that even in the simplest case of solution of parabolized problems the model has 12 differential equations. This fact somewhat diminishes exploitation advantages of the model.

References

[1] B.P. Golovnya, Modeling of the fluctuating component in the form of the sum of an infinite number of random quantities. Part 1. k-ε modelling, Int. J. Heat Mass Transfer (2009), doi:10.1016/j.ijheatmasstransfer.2008.09.046.
[2] J.C. Rotta, Turbulent boundary layers in incompressible flow, Progr. Aerospace Sci. 2 (1962) 1–219.
[3] W. Rodi, On the Equation Governing the Rate of Turbulent Energy Dissipation, Imperial College, Mech. Eng. Rep. TWF/TN/A/41, 1971.
[4] B.J. Daly, F.H. Harlow, Transport equations of turbulence, Phys. Fluids 13 (1970) 26–34.
[5] A.S. Monin, Abut properties of turbulence symmetry in atmospheric boundary layer, Phys. Atmos. Ocean 1 (1) (1965) 45–55.
[6] B.E. Launder, Heat and mass transport, Turbulence. Topics in Applied Physics, vol. 12, Springer-Verlag, New York, 1976. Chapter 6.
[7] R.A.W.M. Henkes, C.J. Hoogendoorn, Comparison of turbulence models for the natural convection boundary layer along a heated vertical plate, Int. J. Heat Mass Transfer 32 (1) (1989) 157–170.
[8] T. Tsuji, Y. Nagano, Turbulence measurements in a natural convection boundary layer along a vertical flat plate, Int. J. Heat Mass Transfer 31 (1989) 2101–2111.
[9] R. Cheeswright, E. Ierokipiotus, Velocity measurements in a turbulent natural convection boundary layer, in: Proc. 7th Int. Heat Transfer Conf., Munich, vol. 2, 1982, pp. 305–309.
[10] A.G. Kirdyashkin, Structure of Thermogravitational Fluxes near Heat Transfer Surface, Ph.D. Thesis, Institute of Thermophysics, Siberian Branch of the USSR Academy of Sciences, Novosibirsk, 1975.
[11] S.S. Kutateladze, Heat Transfer and Hydrodynamic Resistance, Handbook, Nauka Press, Moscow, 1990.
[12] A.G. Darbyshire, T. Mulin, Transition to turbulence in constant-mass-flux pipe flow, J. Fluid Mech. 289 (1995) 83–114.
[13] B. Hof, J. Westerweel, T.M. Schneider, B. Eckhardt, Finite lifetime of turbulence in shear flows, Nature 443 (2006) 59–62.
[14] G. Comte-Bellot, Ecoulement turbulent entre deux parois paralleles, Publ. Sci. Tech. Ministere de l'Air (419) (1965).
[15] R.M.C. So, Y.G. Lai, B.C. Hwang, G.J. Yoo, Low Reynolds number modeling of flows over a backward facing step, ZAMP-39 (1988) 13–27.
[16] J.K. Eaton, J.P. Johnston, Turbulent Flow Reattachment: An Experimental Study of the Flow and Structure behind a Backward-Facing Step, Report No. MD-39, Dept. Mech. Eng., Stamford University, CA, 1980.
[17] D.C. Wilcox, Turbulence Modelling for CFD, DCW Industries, USA, 1994.
[18] D.M. Driver, H.I. Seegmiller, Features of a reattaching turbulent shear layer in divergent channel flow, AIAA J. 31 (1) (1985) 163–171.
[19] B.E. Launder, B.I. Sharma, Application of the energy-dissipation model of turbulence to calculation of flow near a spinning disc, Lett. Heat Mass Transfer 1 (1974) 131–138.
[20] D.C. Wilcox, Reassessment of the scale determining equation for advanced turbulence models, AIAA J. 26 (11) (1988) 1299–1310.
[21] http://www.grc.nasa.gov/WWW/wind/valid/backstep/backstep.html.
[22] F. Menter, Zonal Two-Equation k-ω Turbulence Models for Aerodynamic Flows, AIAA paper 93-2906 (1993).
[23] G.C. Papageorgakis, D.N. Assanis, Comparison of linear and non-linear RNG-based *k*-ε models for incompressible turbulent flow, Numer. Heat Transfer B 35 (1999) 1–22.
[24] J. Kim, S.J. Kline, J.P. Johnston, Investigation of a reattaching turbulent shear layer: flow over a backward-facing step, ASME J. Fluids Eng. 102 (1980) 302–308.
[25] V. Yakhot, S.A. Orszag, Renormalization group analysis of turbulence. 1. Basic theory, J. Sci. Comput. 1 (1986) 3–51.
[26] K.-Y. Chien, Prediction of channel and boundary-layer flows with a low-Reynolds-number turbulence model, AIAA J. 29 (1982) 34–38.
[27] J.C. Rotta, Statistische Theorie nichthomogener Turbulenz, Z. Phys. 129 (1951) 547–572.

[28] M.M. Gibson, B.A. Younis, Calculation of swirling jets with a Reynolds stress closure, Phys. Fluids 29 (1986) 38–48.
[29] B.E. Launder, G.J. Reece, W. Rodi, Progress in the development of a Reynolds stress turbulence closure, J. Fluid Mech. 65 (3) (1975) 537–566.
[30] S. Thangam, C.G. Speziale, Turbulent Separated Flow past a Backward-Facing Step: A Critical Evaluation of Two-Equation Turbulence Models, ICASE Report 91-23, Institute for Computer Applications in Science and Engineering, NASA Langley Research Center, Hampton, Virginia, 1991.
[31] B.E. Launder, Phenomenological modeling: present and future, in: J. Lumley (Ed.), Proc. Ehither Turbulence Workshop, Lecture Notes in Physics, 1990.
[32] A.E. Samuel, P.N. Joubert, A boundary layer developing in an increasingly adverse pressure gradient, J. Fluid Mech. 66 (3) (1974) 481–506.
[33] B.E. Roach, D.H. Brierley, The influence of a turbulent free-stream on zero pressure gradient transitional boundary layer development, in: O. Pirroneau, W. Rodi, I.L. Ryhming, A.M. Savil, T.V. Tuong (Eds.), Numerical Simulation of Unsteady Flows and Transition to Turbulence, C.U.P., New York, 1992, pp. 319–347.
[34] Z. Yang, P.R. Voke, Large-eddy simulation stadies of bypass transition, in: W. Rodi, F. Martelli (Eds.), Engineering Turbulence Modelling in Experiments, vol. 2, Elsevier Science Ltd., Amsterdam, 1993.